Applied Science, Engineering and Management Bulletin [ASEMB]
ISSN: 3049-3005
Vol. 3 No. 02(Apr-June) (2026) |Pg: 94-100

Impact of entropy generation and chemical reaction analysis of nanofluid flow over a linear stretched surface

Rakesh Kumar[1], Naresh Kumar Sharma[2]
[1]Associate Professor, Department of Chemistry, Govt. P. G. Nehru College Jhajjar, Haryana
[2]Professor, Department of Chemistry, Lords University, Alwar, Rajasthan
rakesh.pasrija@gmail.com, nareshamansharma@gmail.com

Abstract

We present a model that analyses entropy generation for the nanofluid flow across a stretched surface with chemical reaction. Determining how entropy growth and chemical reaction affects heat transfer characteristics over a stretching sheet is the aim of this study. The mathematical modeling is characterized by conservation laws of mass, linear momentum, energy, and concentration. It is believed that the presence of nanofluids inhibits the effects of thermophoresis and Brownian motion. Similarity variables are utilised to transform the governing PDE into a nonlinear ODE. The shooting method and RKF approaches were used to numerically solve the ODE. Various factors are used to analyse physical characteristics such as skin friction, temperature, velocity, concentration, Sherwood and Nusselt numbers for stretching. In a restricted sense, a comparison study is conducted with the previously reported results. The main objective while building different thermal devices is to use energy as efficiently as possible. Energy efficiency in thermal engineering operations can be increased by reducing entropy generation.

Keywords: *Entropy generation, Chemical reaction, Nanofluid, Stretching sheet*

Introduction:

Modern engineering and manufacturing processes rely on boundary layer flow over stretched surfaces for a variety of tasks, including cooling metallic sheets in cooling baths, annealing and thinning copper wires, aerodynamic extrusion of plastic and rubber sheets, drawing of plastic films and sheets, production of glass fiber and paper, and many more. The stretching velocity is not always linear, and this is something to keep in mind. Crane [1] did groundbreaking work that laid the groundwork for the dynamics of the movement of a boundary layer across a stretching surface.

Many branches of engineering and business rely heavily on the effects of chemical reactions on heat and mass transport flows. The chemical industry, medicine delivery, magnetic cell separation, subsurface energy transit, and therapy of certain vascular disorders are all greatly impacted by this phenomenon. The chemical reaction has many practical uses in industry and has thus stimulated much research into heat and mass transfer in the scientific and engineering communities [2]. A variety of methods have been investigated to enhance the thermal performance of heat transfer fluids. The incorporation of porous materials is one such technique that significantly improves heat transfer from stretching surfaces in industrial processes [3, 4]. According to Hayat et al. [5], it is considered crucial because of its important function in the design of chemical processing equipment, polymer manufacture, cooling towers, pollution, fog formation and distribution, temperature, fiber insulation, and so on.

For industrial chemical practices, such as oxidation and synthesis of components, processing of food, moisture distribution on cultivated fields, destruction of crops due to cold, and so on, raw materials are constructed to undergo chemical reactions to transform them into advanced standard products. A reactor is used to carry out these kinds of chemical reactions. Chemical reactions involving nanoparticles and conventional liquids can be either homogeneous within a certain phase or heterogeneous outside of that phase's boundary [6]. For first-order chemical reactions, the rate of reaction is proportional to the concentration. Chemical reaction effects on heat and mass transport with varied geometries have been studied and reported by several authors due to their relevance to relevant applications [7-8].

An improvement in thermal conductivity is achieved by dispersing the ultrafine solid metallic particles in technical fluids. When it comes to boosting the coefficient of heat transmission, this is among the most up-to-date and suitable approaches. The phrase "Nano-fluid" was likely first used by Choi and Eastman [9] when they combined nanoparticles with a base fluid. Metals or metal oxides are the most common materials for these particles. We

anticipate that nano-fluids will outperform the base fluid in terms of thermal efficiency since the particles in them have a higher thermal conductivity than the typical fluids used for heat transmission.

Many research in the past relied only on the first rule of thermodynamics when calculating the heat exchanger systems' efficiencies. Multiple competing mechanisms explain for irreversibility in many industrial systems. Refrigeration, heat transmission, storage, solar thermal power conversion, and thermal science teaching are some of the areas where Bejan [10] has extensively discussed entropy generation minimization. Thermal engineering equipment are optimized for greater energy efficiency by employing the entropy generation minimization method. Applying the second rule of thermodynamics to find the optimal thermal system design involves reducing irreversibility [11-12]. The entropy generation function is a way to quantify how many irreversibilities are present in a process, and when these are present, engineering equipment performs worse. Optimal design of energy systems requires reducing entropy generation [13], since this metric measures the available work destruction of the systems. A power production device's useable power cycle outputs decrease while a power consumption device's input to the cycle increases because of entropy creation. Due to the first law's inefficiency in heat transfer engineering systems, the second law of thermodynamics provides more trustworthy results than the first law [14]. To enhance the system's performance, the entropy generation is evaluated. Furthermore, entropy can be generated by heat and mass transport, viscous dissipation, finite temperature gradients, and other similar processes [15].

Motivated by these studies, the present work employs entropy generation analysis based on the second law of thermodynamics to investigate the thermodynamic behavior of the considered heat transfer problem. The study aims to quantify the effects of the governing physical parameters on thermal irreversibility and to identify conditions that minimize entropy generation while maximizing heat transfer efficiency. We have not yet investigated the creation of entropy and the analysis of chemical reactions in nanofluid flow over a linearly stretched surface, which is motivated by the top cited publications. Consequently, the present study's chemical reaction involves generating entropy and transporting heat of the nanofluid past a stretched sheet. The prescribed issue is represented by the governing scheme of the partial differential equations, which are reduced to the non-linear ordinary differential equations via similarity transformations. Computing solutions to the updated equations is done using the shooting method and the Runge Kutta methodology. In the expressions of the tables and graphical profiles, you can see the effects of all the important flow parameters.

Mathematical Formulation:

Consider the steady, two-dimensional boundary layer flow of nanofluid over linear stretching surfaces in the presence of chemical reaction. This model is used for the nanofluid incorporates the effects of thermophoresis and Brownian motion. The co-ordinate system is such that x-axis is taken along the stretching surface in direction of the motion at the origin and the y-axis is perpendicular to the surface of the sheet as shown in Fig. 1. The stretching surface and fluid is maintained at uniform temperature and concentration T_w and C_w and these values are assumed to be greater than the ambient temperature and concentration T_∞ and C_∞ respectively. The sheet at y = 0 is stretched along the x-direction with velocity $u = ax$.

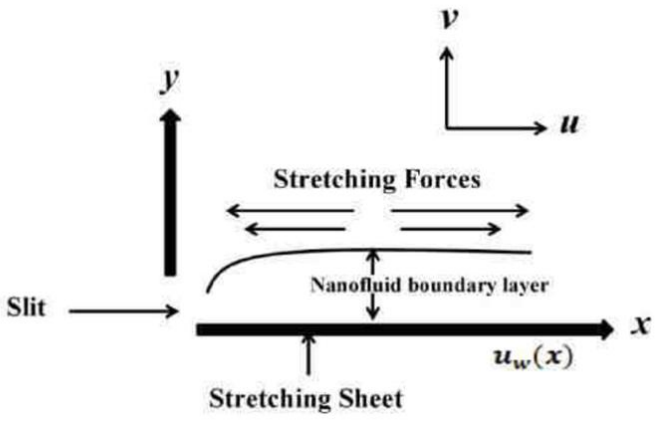

Figure 1. Schematic diagram

The governing equations for the problem are

$$\frac{\partial u}{\partial x}+\frac{\partial v}{\partial y}=0 \tag{1}$$

$$u\frac{\partial u}{\partial x}+v\frac{\partial u}{\partial y}=\nu\frac{\partial^2 u}{\partial y^2} \tag{2}$$

$$u\frac{\partial T}{\partial x}+v\frac{\partial T}{\partial y}=\alpha\frac{\partial^2 T}{\partial y^2}+\tau\left[D_B\frac{\partial C}{\partial y}\frac{\partial T}{\partial y}+\frac{D_T}{T_\infty}\left(\frac{\partial T}{\partial y}\right)^2\right] \tag{3}$$

$$u\frac{\partial C}{\partial x}+v\frac{\partial C}{\partial y}=D_B\frac{\partial^2 C}{\partial y^2}+\frac{D_T}{T_\infty}\frac{\partial^2 T}{\partial y^2}-K_1(C-C_\infty) \tag{4}$$

Boundary Conditions are

$$\left.\begin{array}{ll} u=u_w=ax,\ v=0,\ T=T_w,\ C=C_w & \text{at}\quad y=0 \\ u\to 0,\ T\to T_\infty,\ C\to C_\infty & \text{as}\quad y\to\infty \end{array}\right\} \tag{5}$$

Similarity Variables

$$\left.\begin{array}{l} \eta=\sqrt{\frac{a}{\nu}}y\,,\theta=\frac{T-T_\infty}{T_w-T_\infty},\phi=\frac{C-C_\infty}{C_w-C_\infty} \\ u=axf'(\eta),\ v=-\sqrt{a}f(\eta) \end{array}\right\} \tag{6}$$

The reduced ordinary Differential equations are

$$f'''+ff''-\left(f'^2\right)=0 \tag{7}$$

$$\frac{1}{Pr}\theta''+f\theta'+Nb\,\theta'\phi'+Nt\,(\theta')^2=0 \tag{8}$$

$$\phi''+Lef\phi'+\frac{Nt}{Nb}\theta''-C_r\phi=0 \tag{9}$$

Corresponding Boundary Conditions

$$\left.\begin{array}{l} f(0)=0,f'(0)=1,\theta(0)=1,\phi(0)=1 \\ f'(\infty)=0,\theta(\infty)=0,\phi(\infty)=0 \end{array}\right\} \tag{10}$$

Where

$Nt=\frac{D_T(T_W-T_\infty)}{T_\infty\,\nu}$, $Nb=\frac{D_B(C_W-C_\infty)}{\nu}$, $C_r=\frac{K_1Le}{\alpha}$, $Le=\frac{\nu}{D_B}$ and $Pr=\frac{\nu}{\alpha}$

$C_f=\frac{\tau_w}{\rho\,{u_w}^2}$, $Sh=\frac{xq_m}{D_B(C_W-C_\infty)}$ and $Nu=\frac{xq_w}{k(T_W-T_\infty)}$

Where q_m and q_w are mass flux and heat flux at stretching surface

$$q_m=-D_B(C_w-C_\infty)\sqrt{\frac{a}{\nu}}\phi'(0)$$

$$q_w=-k(T_w-T_\infty)\sqrt{\frac{a}{\nu}}\theta'(0)$$

The volumetric rate of entropy generation in the present of magnetic field is

$$S_G=\frac{k}{T_\infty}\left[\left(\frac{\partial T}{\partial x}\right)^2+\left(\frac{\partial T}{\partial y}\right)^2\right]$$

The first term indicates the entropy generation due to heat transfer across a finite temperature difference, A dimensionless number for entropy generation rate N_S is defined as the ratio of the local volumetric entropy generation rate S_G to a characteristic entropy generation rate $(S_G)_0$. For a prescribed boundary condition the characteristic entropy generation rate is

$$(S_G)_0 = \frac{k\,\Delta T^2}{x^2 {T_\infty}^2}$$

Hence, the entropy generation number is

$$N_S = \frac{S_G}{(S_G)_0}$$

Using Above equations, it can be expressed as

$$N_S = \left(\theta'(0)\right)^2$$

Numerical Procedure:

Using Runge-Kutta-Fehlberg's fourth and fifth order methods with the assistance of shooting technique, the non-linear ordinary differential equations (7) to (9) have been solved for the frontier scenarios (10). Here are the steps involved in the methodology: At the outset, the dominant system of equations (7) through (9) was reduced to a system of differential equations of initial order by introducing the most recent dependant variable. Assisting shooting strategies identified outstanding missed beginning situations in the systems of initial ordered differential equations, which identify basic conditions. Following that, in the same way, all the conditions for the far field frontier were eventually met, and a finite value for η∞ is chosen. The massive computations were determined by the quantity close to $\eta_\infty = 10$, which is sufficient to asymptotically achieve the far fields frontier requirements for all parameters considered. The Runge-Kutta-Fehlbergs-45 algorithm was used to accomplish integration after fixing finite quantities for η_∞. When the correct stepsize h was being used, Runge-Kutta-Fehlbergs-45 technique has the processes to determine it. Two different approximations of the solutions are made and compared at each stage. The approximations are established when the two responses are in closed agreements; otherwise, the step sizes are reduced until the requisite accuracy is achieved. In this study, we assume a $\Delta\eta = 0.001$ step size, far fields frontier requirements close to $\eta_\infty = 10$, and precision to the fifth decimal place. The procedure is represented by flow chart in figure 2

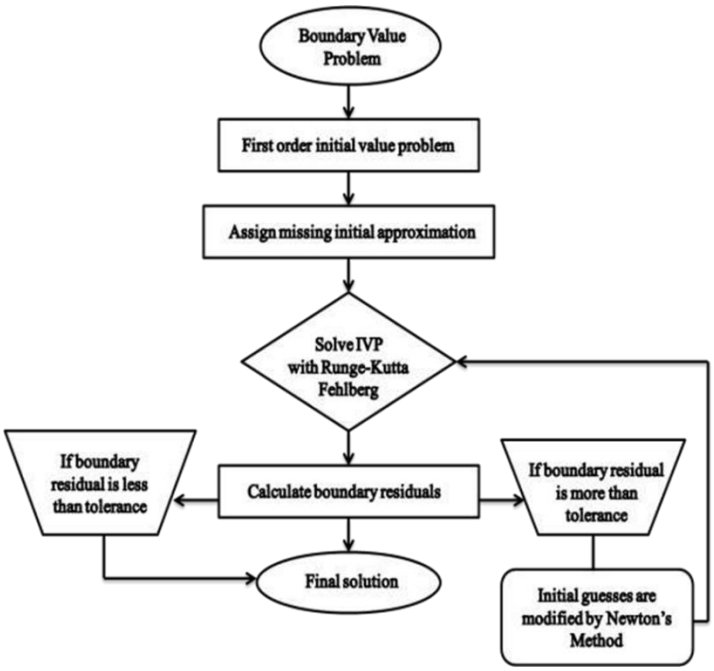

Figure 2. Flow Chart of Numerical Procedure

Results and Discussion:

Figure 3 illustrates the effect of the thermophoresis parameter Nt on the concentration profile. It is observed that the nanoparticle concentration increases with increasing values of Nt . Physically, thermophoresis refers to the migration of nanoparticles from regions of higher temperature to regions of lower temperature under the influence

of a temperature gradient. As the thermophoresis parameter increases, a larger number of nanoparticles are transported away from the heated stretching surface into the fluid. This enhanced migration leads to the accumulation of nanoparticles within the concentration boundary layer, thereby increasing the nanoparticle concentration throughout the flow domain. Consequently, the concentration boundary layer becomes thicker, resulting in higher concentration profiles for larger values of the thermophoresis parameter.

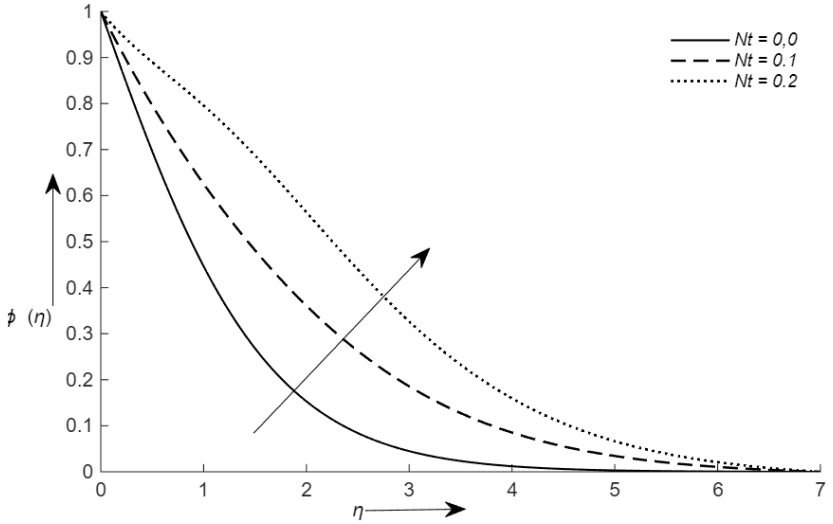

Figure 3. Concentration profile for Nt

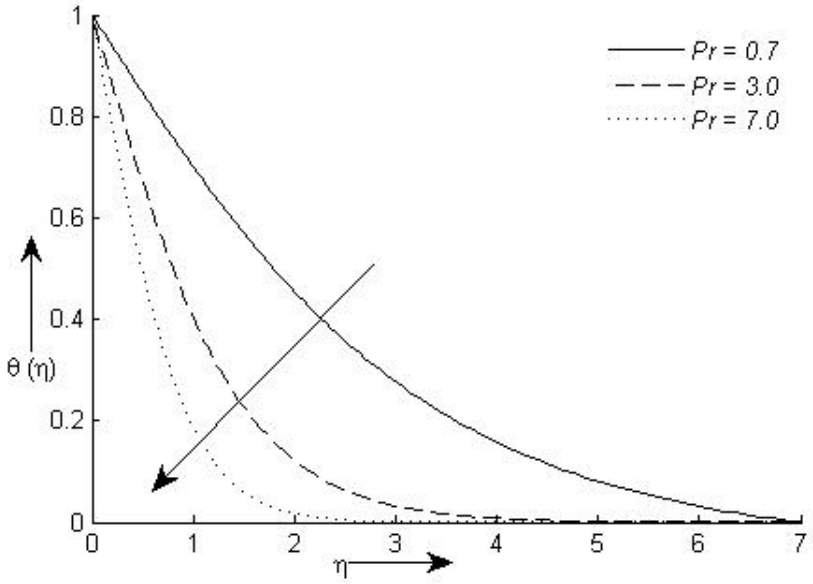

Figure 4. Temperature profile for Pr

Figure 4 depicts the influence of the Prandtl number Pr on the temperature profile. It is observed that the temperature decreases with increasing values of the Prandtl number. Physically, the Prandtl number represents the ratio of momentum diffusivity (kinematic viscosity) to thermal diffusivity. A higher value of Pr corresponds to lower thermal diffusivity, indicating that heat diffuses more slowly through the fluid. As a result, thermal energy remains confined to a thinner region adjacent to the stretching surface, leading to a reduction in both the thermal boundary layer thickness and the fluid temperature. Therefore, fluids with higher Prandtl numbers exhibit lower temperature distributions compared to fluids with lower Prandtl numbers. This behavior is typical of fluids such as oils, which possess relatively low thermal diffusivity, whereas fluids with low Prandtl numbers, such as liquid metals, allow heat to diffuse more rapidly, resulting in higher temperature profiles.

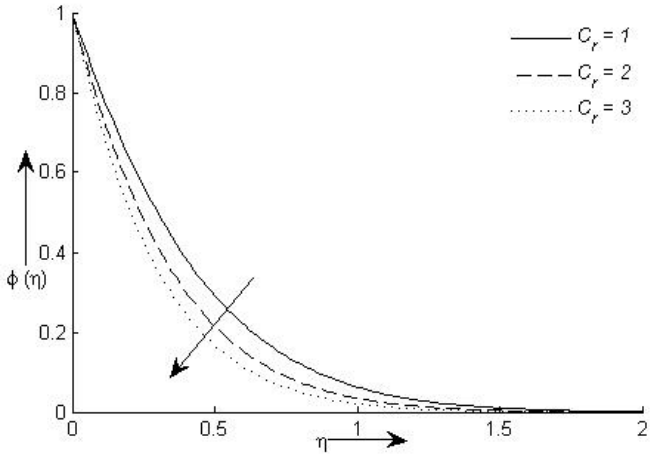

Figure 5. Concentration profile for C_r

Figure 5 illustrates the influence of the chemical reaction parameter C_r on the concentration profile. It is evident that the concentration decreases as the value of C_r increases. Physically, a higher chemical reaction parameter signifies a stronger destructive (consumptive) chemical reaction, which accelerates the consumption of the diffusing species within the boundary layer. Consequently, the concentration of the species decreases throughout the flow region. The intensified chemical reaction reduces the concentration boundary layer thickness by depleting the species more rapidly than it can diffuse from the surface. Therefore, increasing the chemical reaction parameter suppresses the concentration distribution and leads to a thinner concentration boundary layer. This behavior confirms that stronger chemical reactions enhance mass transfer by reducing the concentration of the diffusing species in the fluid.

Conclusion

The present study is to find out numerical solution of chemical reaction analysis of nanofluid flow over a linear stretched surface. The RK method has been applied to find out the impact of various physical conditions. The graph represents the performance of dimensionless temperature, and concentration profiles over the different dimensionless parameters. The important outline of this study is explained below:

1. An increase in the thermophoresis parameter enhances the nanoparticle concentration within the boundary layer. Stronger thermophoretic forces transport nanoparticles from the heated surface toward cooler regions, resulting in a thicker concentration boundary layer.

2. The temperature profile decreases with increasing Prandtl number due to the reduction in thermal diffusivity. Higher values of lead to a thinner thermal boundary layer, thereby reducing the temperature distribution throughout the fluid.

3. Increasing the chemical reaction parameter suppresses the concentration profile by accelerating the consumption of the diffusing species. Consequently, the concentration boundary layer becomes thinner, indicating enhanced mass transfer due to stronger chemical reactions.

References:

[1] L. J. Crane, “Flow past a stretching plate,” Zeitschrift für Angewandte Mathematik und Physik, vol. 21, pp. 645–647, 1970.
[2] T. Hayat, M. Waqas, S. Shehzad, and A. Alsaedi, “Chemically reactive flow of third grade fluid by an exponentially convected stretching sheet,” Journal of Molecular Liquids, vol. 223, pp. 853–860, 2016.
[3] E. M. A. Elbashbeshy and M. A. A. Bazid, “Heat transfer over an unsteady stretching surface,” Heat and Mass Transfer, vol. 41, no. 1, pp. 1–4, 2004.
[4] V. Poply, “Effect of varying thermal conductivity and viscosity in unsteady free stream flow over stretching sheet,” Bulletin of Pure & Applied Sciences–Mathematics and Statistics, vol. 37, no. 2, pp. 260–266, 2018.
[5] T. Hayat, M. Waqas, S. A. Shehzad, and A. Alsaedi, “On 2D stratified flow of an Oldroyd-B fluid with chemical reaction: An application of non-Fourier heat flux theory,” Journal of Molecular Liquids, vol. 223, pp. 566–571, 2016.

[6] A. A. Afify, “MHD free convective flow and mass transfer over a stretching sheet with chemical reaction,” Heat and Mass Transfer, vol. 40, no. 6, pp. 495–500, 2004.
[7] M. Ramzan, M. Bilal, and J. D. Chung, “Radiative Williamson nanofluid flow over a convectively heated Riga plate with chemical reaction—A numerical approach,” Chinese Journal of Physics, vol. 55, no. 4, pp. 1663–1673, 2017.
[8] P. Sreedevi, P. Sudarsana Reddy, and A. J. Chamkha, “Heat and mass transfer analysis of nanofluid over linear and non-linear stretching surfaces with thermal radiation and chemical reaction,” Powder Technology, vol. 315, pp. 194–204, 2017.
[9] S. U. S. Choi and J. A. Eastman, “Enhancing thermal conductivity of fluids with nanoparticles,” Materials Science, vol. 231, pp. 99–105, 1995.
[10] A. Bejan, *Entropy Generation Minimization: The Method of Thermodynamic Optimization of Finite-Size Systems and Finite-Time Processes*. Boca Raton, FL, USA: CRC Press, 1996.
[11] A. Bejan, “Second-law analysis in heat transfer and thermal design,” iAdvances in Heat Transfer, vol. 15, New York, NY, USA: Elsevier, 1982, pp. 1–58.
[12] O. Mahian, S. Mahmud, and S. Z. Heris, “Analysis of entropy generation between co-rotating cylinders using nanofluids,” Energy, vol. 44, pp. 438–446, 2012.
[13] A. Bejan, “Second law analysis in heat transfer,” Energy, vol. 5, pp. 720–732, 1980.
[14] H. F. Oztop and K. Al-Salem, “A review on entropy generation in natural and mixed convection heat transfer for energy systems,” Renewable and Sustainable Energy Reviews, vol. 16, pp. 911–920, 2012.
[15] S. Aïboud and S. Saouli, “Second law analysis of viscoelastic fluid over a stretching sheet subject to a transverse magnetic field with heat and mass transfer,” Entropy, vol. 12, pp. 1867–1884, 2010.